

# Transport and phase transition of active Brownian particles in rearranging heterogeneous environments modelled diffusing activity

S. M. J. Khadem<sup>1</sup>, N. H. Siboni<sup>1</sup> and S. H. L. Klapp<sup>1</sup>  
<sup>1</sup>*Institut für Theoretische Physik, Technische Universität Berlin,  
Hardenbergstraße 36, 10623 Berlin, Germany*

(Dated: March 1, 2025)

In this work, we study the dynamics of a single active Brownian particle and the collective behavior of interacting active particles in evolving heterogeneous media. We apply the idea of the diffusing diffusivity model to mimic the environmental heterogeneity in the equation of motion of the active particle via time-dependent activity and diffusivities. In our model, the fluctuations of environment simultaneously and similarly affect the motility and diffusion coefficients. We obtain the probability distribution function of particle displacement and its moments analytically and support our data via particle-based simulations. We finally investigate the impact of the introduced fluctuations on the collective behavior of active Brownian particles. Our results show that these fluctuations hinder the motility-induced phase separation, together with a significant change of the density dependence of particle velocities.

## I. INTRODUCTION

Transport of a passive particle in the complex heterogeneous systems such as crowded biological media, porous material or polymeric networks can strongly be modified and differ from the normal diffusion of a particle in a simple fluid. Normal diffusion is characterised by a Gaussian probability distribution together with a mean squared displacement (MSD) which linearly grows in time. An often observed phenomenon in such complex systems is the anomalous diffusion of a tracer particle described by a nonlinear MSD associated with either a Gaussian or non-Gaussian probability distribution. To explain the observed anomalies, different physical models based on different physical assumptions have been proposed. These models rely on very different mathematical tools, being the generalizations of the Einstein's and Langevin's approaches [1].

In many heterogeneous systems, the particle experiences different diffusivities over time. This is either due to the evolution of the medium by its own or the motion of the particle in regions with different diffusivities. Such situations have been observed in numerous single particle tracking experiments for widely different types of tracer particles and the media [2–5] as well as simulation studies [6, 7]. In these studies it is shown that while the mean square displacement of the passive particle remains linear, its displacement probability density function (PDF) deviates from the Gaussian form at short times. These observations were in contradiction with Fick's second law, where the displacement PDF of particle displacement in normal diffusion obeys the standard diffusion equation and has a Gaussian form at all times. These observations suggested the development of a new class of stochastic processes and were referred to as 'Brownian yet non-Gaussian' [8].

This new dynamics was first theoretically explained by the classical idea of the superstatistics [9] where the single Gaussian distribution is averaged over exponential distribution of diffusivities  $p(D)$  [4]. Another approach termed

as 'diffusing diffusivity' was proposed [10–12] assuming that the diffusivity of the particle constantly changes according to a specific random process. Diffusing diffusivity model was further studied with respect to time averages and ergodicity breaking properties [13]. It was also compared with the concept of the generalized Grey-Brownian motion with random diffusivity [14]. An elegant formalism of the diffusing diffusivity model using the subordination approach was later put forward in Ref. [15], which connected the superstatistics approach with the diffusing diffusivity model. We note that the dynamics of the 'Brownian yet non-Gaussian' process could be reproduced by the continuous time random walk model in equilibrium with a truncated heavy tailed waiting time PDF [16].

Similar to the case of passive particles, active particles (AP) are also often found in heterogeneous environment at all length scales. Examples might include molecular motors in the crowded environment inside the cells [17], bacteria in highly complex tissues [18] or herds of animals migrating in forest [19]. It is shown that most of the non-equilibrium features of the collective behavior of APs and their individual dynamics are strongly affected, when they take place in heterogeneous media [20–22]. Different phenomena such as anomalous diffusion of AP in random Lorentz gas [23] and trapping of APs in the presence of obstacle arrays [24], avalanche dynamics transport of run-and-tumble [25] or Clogging and depinning of ballistic active matter [26] at macro-scale, were observed which are absent when the medium is homogeneous. Thus, it is crucial to include the environmental heterogeneities in modeling the collective behavior of APs as well as their individual dynamics. One should note that the observed phenomena depends on the type of the AP and also the characteristics of the heterogeneity in the environment, See Ref. [27] for a review.

Motivated by aforementioned theoretical works which have been restricted to systems with passive particles, here we investigate the dynamics of APs in evolving heterogeneous systems. In particular, investigate the im-

part of the fluctuations of the activity, rotational and translational diffusion coefficients on the dynamics of active Brownian particles (ABP) [28, 29]. We have chosen the ABP model as it is one of the most popular models for description of the APs [28, 29]. The ABP model is used to explain the experimentally observed dynamics of self-propelled particles [29–31] and also to describe the collective behaviors of the colloids and bacteria [27]. For the modified ABPs, we study the behavior of MSD and PDF of particle displacement with a reference to the dynamics of ABPs in a homogeneous medium. Introduction of these fluctuations in dynamics of ABPs are particularly interesting, as well as essential, as the evolution of the natural biological medium introduces another time-scale into problem. We proceed to study the effect of these fluctuations on the collective behavior of the system. Noting that the rotational diffusion and the motility play essential roles in the emergence of MIPS, introducing fluctuations in these parameters can have a considerable impact on the occurrence of MIPS. We quantify these modification via obtaining the phase diagram and the correlation between the particle velocity and the local density.

## II. SINGLE ACTIVE BROWNIAN PARTICLE WITH FLUCTUATIONS

In this section, we commence by a brief review of the ABP model in homogeneous environment (which we refer to as the conventional ABP model). We continue by building up a model for an ABP via introducing fluctuations into the conventional description of ABP. We then analytically investigate the effect of these fluctuations on the PDF of the displacements and the MSD of the fluctuating ABPs, using sub-ordination approach. Finally, we support our theoretical predictions by extensive simulation results.

### A. Conventional Active Brownian Particle

In ABP model, the particles exhibit directed motions in addition to the Brownian motion. These directed motions may arise from a self-propulsion force,  $F_0$ , which is (typically) directed along an anisotropy axes of the particle (i.e. heading vector). Due to the thermal fluctuations, the particle experiences translational  $\xi_T(t)$  and rotational  $\xi_R(t)$  noises which affect its position ( $\mathbf{r}$ ) and orientation ( $\phi$ ), respectively. The ABP model may thus be described by the following Langevin equations

$$\begin{aligned}\gamma_T \dot{\mathbf{r}}(t) &= F_0 \hat{\mathbf{e}}(t) + \sqrt{2k_B T \gamma_T} \xi_T(t) \\ \gamma_R \dot{\phi}(t) &= \sqrt{2k_B T \gamma_R} \xi_R(t),\end{aligned}\tag{1}$$

where the vector  $\hat{\mathbf{e}}(t) := (\cos \phi, \sin \phi)$  determines the heading direction of the particle. The parameters  $\gamma_T = 6\pi\eta R$  and  $\gamma_R = 8\pi\eta R^3$  denote the translation and rotational Stokes friction coefficients, respectively [27], with  $\eta$  being the viscosity and  $R$  the radius of the particle. The noise terms are Gaussian white noises satisfying  $\langle \xi_T(t) \rangle = 0$ ,  $\langle \xi_R(t) \rangle = 0$ ,  $\langle \xi_{T,j}(t_1) \xi_{T,i}(t_2) \rangle = \delta(t_1 - t_2) \delta_{i,j}$ , and  $\langle \xi_R(t_1) \xi_R(t_2) \rangle = \delta(t_1 - t_2)$ . The parameters  $k_B T$  and  $k_B T_R$  are the effective thermal energies which quantify the strength of the translational and the rotational noises, respectively [32]. In many applications [33–36], it is assumed that  $T = T_R$  and therefore, the rotational and the translational diffusion coefficients are written as  $D_R = k_B T / (8\pi\eta R^3)$ , and  $D_T = k_B T / (6\pi\eta R)$ , both are proportional to  $\eta^{-1}$ . Similarly, the motility of the ABP defined as  $v_0 = F_0 / \gamma_T = F_0 / (6\pi\eta R)$  is also proportional to  $\eta^{-1}$ .

The conventional ABP model assumes that the medium in which the AP moves is homogeneous and has a viscosity which is constant over all length-scales, i.e.  $\eta(\mathbf{r}) = \eta$ . This leads to constant translational and rotational diffusivities, i.e.  $D_{T,R}(\mathbf{r}) = D_{T,R}$ , and motility  $v_0(\mathbf{r}) = v_0$ .

### B. Active Brownian particle with fluctuations

Here, we relax the aforementioned condition by considering an ABP model whose characteristic parameters are not anymore constant. A justification of this case could be to consider a heterogeneous environment whose viscosity varies in space  $\eta = \eta(\mathbf{r})$ . In such an environment, the diffusing particle experiences different viscosities while diffusing in the medium. Essentially in such a system, the particle would need a certain time to sample the existing heterogeneity. For the measurements with time laps longer than this time, one would recapture the conventional ABP model with (averaged) constant parameters. However, when the measurement time interval is shorter, the spatial variation of  $\eta$  needs to be inserted in the equation of the motion of the particle.

#### 1. Model

One approach to model this system is to exploit the idea of the diffusing diffusivity model, that is, the spatial heterogeneity of an evolving medium may be *mimicked* by a time dependent stochastic process. In our case, the characteristic parameter is  $\eta(\mathbf{r})$  which we set to be calculated from a random process, say  $\mathcal{Y}^{-1}(t)$ . This implies that the friction coefficients at time  $t$  are proportional to the process  $\mathcal{Y}(t)$ ;  $\gamma_{T,R}(t) \propto \mathcal{Y}(t)^{-1}$ . Rewriting the Eq. 1

in the following form

$$\begin{aligned}\dot{\mathbf{r}}(t) &= \frac{F_0}{\gamma_T(t)}\hat{\mathbf{e}}(t) + \sqrt{\frac{2k_B T}{\gamma_T(t)}}\boldsymbol{\xi}_T(t) \\ \dot{\phi}(t) &= \sqrt{\frac{2k_B T}{\gamma_R(t)}}\xi_R(t),\end{aligned}$$

it becomes evident that the environmental fluctuations (through  $\gamma_{R,T}(t)$ ) affect the motility and diffusivities simultaneously and similarly. Thus one gets the relation below between these quantities

$$D_R(t)/D_R^* = D_T(t)/D_T^* = v_0(t)/v^* = \Upsilon(t) \quad (2)$$

where  $\Upsilon(t)$  is constrained to be positive. The modified Langevin equations of motion of the ABP may then be rewritten as follows:

$$\begin{aligned}\dot{\mathbf{r}}(t) &= v^*\Upsilon(t)\hat{\mathbf{e}}(t) + \sqrt{2D_T^*\Upsilon(t)}\boldsymbol{\xi}_T(t) \\ \dot{\phi}(t) &= \sqrt{2D_R^*\Upsilon(t)}\xi_R(t).\end{aligned} \quad (3)$$

We note that the introduced fluctuations in this work are considered to be external. This differs from the internal fluctuations which were considered in Ref. [37] where the fluctuations in the motility are not correlated to fluctuations in the direction of motion.

A direct consequence of the Eq. 3 is that, despite the time dependency of the motility and the diffusion coefficients, the Peclet number assigned to the motion of the particle is a constant and does not vary in time, i.e.  $Pe = \frac{v_0(t)}{\sqrt{D_R(t)D_T(t)}} = \frac{v_0}{\sqrt{D_R^*D_T^*}}$ . With these assumptions, the rotational diffusion coefficient and the motility are synchronized and consequently the persistent length of the ABP remains constant. Thus, in a coarse-grained picture, the fluctuating model exactly reproduces the ordinary ABP model. Therefore one would expect the emergence of a normal diffusion behavior of MSD accompanied by a Gaussian form of the propagator at times longer than the rotational relaxation time.

An equivalent representation of Eq. 3 is provided by the Fokker-Plank equation for the PDF of the particle displacement and orientation,  $P(\mathbf{r}, \phi, t)$ , which yields:

$$\begin{aligned}\partial_t P(\mathbf{r}, \phi, t) &= -\Upsilon(t)v^*\hat{\mathbf{e}}(t)\cdot\nabla P + \Upsilon(t)D_T^*\Delta P \\ &+ \Upsilon(t)D_R^*\partial_\phi^2 P,\end{aligned} \quad (4)$$

with  $\nabla = \frac{\partial}{\partial x}\hat{i} + \frac{\partial}{\partial y}\hat{j}$  and  $\Delta = \frac{\partial^2}{\partial x^2} + \frac{\partial^2}{\partial y^2}$ . This equation and Eq. 3 provide a toolbox for studying the dynamic of an ABP in an evolving environment where the dynamics of the evolution is estimated by the stochastic process  $\Upsilon(t)$ . In what follows, we perform a throughout analysis of the dynamics of the particle by using the subordination method [38] for solving Eq. 4.

## 2. Sub-ordination

Sub-Ordination is a strong mathematical technique to describe complex stochastic processes [38] (see Refs. [39, 40] for examples). Chechkin et al [15] extended the notion of the sub-ordination to the problem of the diffusing diffusivity of a passive Brownian particle by connecting the diffusivity to the random time increment of the original Brownian motion. Inspired by this work, we rewrite the Eq. 4 in the subordinated form:

$$\begin{aligned}\partial_u P(\mathbf{r}, \phi, u) &= -v^*\hat{\mathbf{e}}(u)\cdot\nabla P + D_T^*\Delta P + D_R^*\partial_\phi^2 P \\ \frac{\partial u}{\partial t} &= \Upsilon(t)\end{aligned} \quad (5)$$

where  $P(\mathbf{r}, \phi, u)$  is the PDF of the particle displacement and orientation corresponding to an ordinary ABP described by Eq. 1. The Fokker-Plank equation above corresponds to the Langevin equation of the motion of the modified ABP whose subordinated form reads as

$$\begin{aligned}\dot{\mathbf{r}}(u) &= v^*\hat{\mathbf{e}}(u) + \sqrt{2D_T^*}\boldsymbol{\xi}_T(u) \\ \dot{\phi}(u) &= \sqrt{2D_R^*}\xi_R(u) \\ \frac{\partial u}{\partial t} &= \Upsilon(t).\end{aligned} \quad (6)$$

Having these equations of the motion at hand with a known  $\Upsilon(t)$ , one can calculate the desired quantities, namely the PDF of particle displacement and its moments.

## 3. PDF of displacement and moments

The standard solution of the subordinated equation, Eq. 5, reads as

$$P(\mathbf{r}, \phi, t) = \int_0^\infty \Upsilon(u, t)G(\mathbf{r}, \phi, u)du, \quad (7)$$

with  $\Upsilon(u, t)$  being the probability density function of the process  $u(t) = \int_0^t \Upsilon(t')dt'$ . Here We focus on the coarse-grained PDF of particle displacement. Integrating both sides of the Eq. 7 over  $\phi$ , one obtains  $P(\mathbf{r}, t) = \int_0^\infty \Upsilon(u, t)G(\mathbf{r}, u)du$  whose Fourier transformation yields:

$$\hat{P}(\mathbf{k}, t) = \int_0^\infty \Upsilon(u, t)\hat{G}(\mathbf{k}, u)du. \quad (8)$$

Since an analytical form of  $G(\mathbf{r}, u)$ , also  $\hat{G}(\mathbf{k}, u)$ , is not available, one can obtain the approximate asymptotic behavior by substituting the Fourier transform of the PDF of displacement for the ordinary ABP for  $\hat{G}(\mathbf{k}, u)$ . From Ref. [41], it is known that  $\hat{G}(\mathbf{k}, u)$  has the following form:

$\hat{G}(\mathbf{k}, u) \sim e^{-D'k^2 u}$  as  $k \frac{v^*}{D_R^*} \rightarrow 0$  with  $D' = \frac{v^{*2}}{2D_R^*} + D_T^*$  and  $k = |\mathbf{k}|$  [41]. Thus one can obtain the asymptotic behavior of the displacement PDF for the fluctuating particle as

$$\begin{aligned} \hat{P}(\mathbf{k}, t) &= \int_0^\infty \Upsilon(u, t) \hat{G}(\mathbf{k}, u) du \\ &\sim \int_0^\infty \Upsilon(u, t) e^{-D'k^2 u} du \\ &= \hat{\Upsilon}(D'k^2, t) \end{aligned} \quad (9)$$

with  $\hat{\Upsilon}$  being the Laplace transform of the kernel  $\Upsilon(s, t) = \int_0^\infty \Upsilon(u, t) e^{-su} du$  with  $s = D'k^2$ . The condition of  $k \frac{v^*}{D_R^*} \rightarrow 0$  implies that the results for  $P(r, t)$  obtained by taking the inverse Fourier transform of  $\hat{T}(D'k^2, t)$  will be valid only at distances larger than the persistent length of the motion, i.e. for  $r \gg \frac{v^*}{D_R^*}$ .

The aforementioned approximation is not required if one is interested in the moments of the PDF. In this case, one can obtain exact expressions for the moments of the PDF at all times, provided that the moments of  $G(\mathbf{r}, u)$  could be calculated by direct integration of the first two lines in Eq. 6. Recalling that the  $m$ -moment of the PDF can be calculated as  $\langle \mathbf{r}^m(t) \rangle = (-i)^n \nabla_{\mathbf{k}}^m \hat{P}(\mathbf{k}, t)|_{\mathbf{k}=0}$ , one can apply the operator above on the  $\mathbf{k}$ -dependent quantities in the both sides of Eq. 8, and immediately arrive at the relation between the moments of the PDF in fluctuating and ordinary ABP model, i.e. between  $\langle \mathbf{r}^m(t) \rangle$  and  $\langle \mathbf{r}_0^m(t) \rangle$  as

$$\langle \mathbf{r}^m(t) \rangle = \int_0^\infty \Upsilon(u, t) \langle \mathbf{r}_0^m(u) \rangle du \quad (10)$$

which has the same form of transformation for PDFs of the both processes. For an ordinary ABP, one can show that the mean squared displacement reads [41]

$$\begin{aligned} \langle \mathbf{r}_0^2(u) \rangle &= \frac{4v^{*2}}{D_R^{*2}} \left[ \left( \frac{D_R^* D_T^*}{v^{*2}} + \frac{1}{2} \right) D_R^* u \right. \\ &\quad \left. - \frac{1}{2} (1 - e^{-D_R^* u}) \right] \end{aligned} \quad (11)$$

which exhibits two crossovers from diffusive behavior to the ballistic one and vice versa.

Let us now substitute Eq. 11 in Eq. 10 and calculate the MSD of the fluctuating ABP:

$$\begin{aligned} \langle \mathbf{r}^2(t) \rangle &= \frac{4v^{*2}}{D_R^{*2}} \left[ \left( \frac{D_R^* D_T^*}{v^{*2}} + \frac{1}{2} \right) D_R^* \left( \int_0^\infty \Upsilon(u, t) u du \right) \right. \\ &\quad \left. - \frac{1}{2} \left( \int_0^\infty \Upsilon(u, t) du - \int_0^\infty \Upsilon(u, t) e^{-u D_R^*} du \right) \right] \\ &= \frac{4v^{*2}}{D_R^{*2}} \left[ \left( \frac{D_R^* D_T^*}{v^{*2}} + \frac{1}{2} \right) D_R^* \langle u(t) \rangle \right. \\ &\quad \left. - \frac{1}{2} (1 - \hat{\Upsilon}(D_R^*, t)) \right]. \end{aligned} \quad (12)$$

The first integral  $\langle u \rangle = \int_0^\infty \Upsilon(u, t) u du$ , being the first moment of  $\Upsilon$ , could be solved using the first derivative of its Laplace transform  $\hat{\Upsilon}(s, t)$  with respect to  $s$  at  $s = 0$ , i.e.  $\langle u \rangle = -\frac{\partial \hat{\Upsilon}(s, t)}{\partial s} \Big|_{s=0}$ . While the result of the second integral is unity, due to the normalization of the PDF, the third integral  $\int_0^\infty \Upsilon(u, t) e^{-u D_R^*} du$  equals essentially to the local value of the Laplace transform of the kernel at  $s = D_R^*$ . Similarly, one can continue these calculations for higher values of  $m$  and calculate parameters such as reduced-kurtosis and compare them with those for the ordinary ABP model in order to study the impact of the fluctuations on the dynamic of the process. Similarly, one can continue these calculations for higher values of  $m$  and calculate parameters such as reduced-kurtosis and compare them with those for the ordinary ABP model in order to study the impact of the fluctuations on the dynamic of the process.

#### 4. fluctuations and results

We now shall return to the process  $\Upsilon(t)$ , which encodes all the information regarding the fluctuations of the environment. Following the suggestions by Jain et al. [11] and Chechkin et al. [15], we consider the viscosity in our model to be the square of a  $n$ -dimensional Ornstein-Uhlenbeck process, i.e.  $\Upsilon(t) = \mathbf{Y}_n^2(t)$ , where  $\mathbf{Y}_n$  is essentially the position vector of an imaginary  $n$ -dimensional harmonic oscillator that performs Brownian motion. With this Ansatz, one obtains the following Langevin equation,

$$\begin{aligned} \Upsilon(t) &= \mathbf{Y}_n^2(t) \\ \dot{\mathbf{Y}}(t) &= -\frac{1}{\tau_o} \mathbf{Y}(t) + \sigma \zeta(t). \end{aligned} \quad (13)$$

where  $\zeta$  is the Gaussian white noise with zero mean and the correlation function of  $\langle \zeta_i(t_1) \zeta_j(t_2) \rangle = \delta_{ij} \delta(t_1 - t_2)$  for  $i, j = 1, \dots, n$ . The parameters  $\sigma$  and  $\tau_o$  denote the characteristic parameters for the imaginary Brownian harmonic oscillator. The auxiliary variable  $\mathbf{Y}$  is a dimensionless parameter and the physical dimensions of  $\sigma$  and  $\tau_o$  are  $[\sigma] = s^{-1/2}$  and  $[\tau_o] = s$ . The parameter  $\tau_o$  determines the time scale below which the fluctuations are dominant and above which the ordinary behavior of the ABP emerges.

*Equilibrium initial conditions:* The choice of the initial condition for the process  $\mathbf{Y}$ , as the sub-ordinator process, can alter the dynamics of the particle at short times [14]. Equilibrium initial conditions corresponds to the case where the measurement starts long after the process  $\mathbf{Y}$  has reached its stationary state. Therefore the initial value  $\mathbf{Y}_0$  should randomly be taken from the equilibrium Boltzmann distribution of the process  $\mathbf{Y}$ . The mean value of  $\Upsilon$  is then determined by the stationary auto-correlation of Ornstein-Uhlenbeck being  $\langle \Upsilon_{st} \rangle = \langle \mathbf{Y}_{st}^2 \rangle = \frac{n\sigma^2 \tau_o}{2}$  for  $t \gg \tau_o$ . For such a choice of the initial conditions, the form of the PDF,  $\Upsilon_n^{eq}(u, t)$ , for

the process  $u(t) = \int_0^t \Upsilon(t') dt'$  has the following form in the Laplace domain [42],

$$\hat{\Upsilon}_n^{eq}(s, t) = \exp\left(\frac{nt}{2\tau_o}\right) / \left[\frac{1}{2}(\sqrt{1 + 2s\sigma^2\tau_o^2} + \frac{1}{\sqrt{1 + 2s\sigma^2\tau_o^2}})\right] \times \sinh\left(\frac{t}{\tau_o}\sqrt{1 + 2s\sigma^2\tau_o^2}\right) + \cosh\left(\frac{t}{\tau_o}\sqrt{1 + 2s\sigma^2\tau_o^2}\right)]^{n/2}. \quad (14)$$

The quantity  $\langle u \rangle$  can now be readily calculated as  $\langle u \rangle = -\frac{\partial \hat{\Upsilon}_n^{eq}(s, t)}{\partial s} \Big|_{s=0} = \frac{n\sigma^2\tau_o}{2} t$  which leads to the following expression for the MSD of the fluctuating ABP

$$\langle r^2(t) \rangle = 4\bar{D}_T t + 2\frac{\bar{v}^2}{\bar{D}_R^2} (\bar{D}_R t - 1 + \hat{\Upsilon}(D_R^*, t)) \quad (15)$$

where  $\bar{D}_T = \frac{n\sigma^2\tau_o}{2} D_T^*$ ,  $\bar{D}_R = \frac{n\sigma^2\tau_o}{2} D_R^*$  and  $\bar{v} = \frac{n\sigma^2\tau_o}{2} v^*$  represent the stationary values of the diffusivities and the motility.

Fig.1 shows the plotted MSD according to Eq. 15 for the set of parameters of  $v^* = D_R^* = \sigma = \tau_o = 1$  and  $D_T^* = 0.1$  together with the corresponding simulation results. The simulation details can be found in Sec. III. As seen in Fig.1, the behavior of the MSDs at very short and long times (with respect to  $\bar{\tau}_R = \frac{1}{\bar{D}_R}$ ) matches with the asymptotic behavior of the MSD of the conventional ABP, that is a linear growth of the MSD with respect to time. This phenomenon that the linear part of MSD remains unchanged under fluctuations, is in agreement with the case of the passive Brownian particle, widely studied in the context of diffusing diffusivity problem. At the intermediate times, however, a slight difference between the MSD of the fluctuating and that of the conventional ABP is observed. Qualitatively one observes that the ballistic behavior of MSD of the conventional ABP is substituted by a smooth cross-over when the fluctuations are introduced. The difference between two MSDs is however slight and can be neglected in the presence of whatever experimental noise. The ratio of these two MSDs is plotted as sub-set in Fig.1. This graph suggests that for higher dimensions of the subordinator process,  $n > 1$ , the observed difference becomes more insignificant.

As we proceed to show, the dynamic of the MSD changes when the time scales corresponding to the fluctuations and rotational relation time deviate from each other. In Fig.2, we plot the MSD of the fluctuating ABP according to Eq. 15 for different values of  $\bar{\tau}_R = \frac{1}{\bar{D}_R}$ , being i)  $\bar{\tau}_R \ll \tau_o$ , ii)  $\bar{\tau}_R = \tau_o$  and iii)  $\bar{\tau}_R \gg \tau_o$ . The first two cases are very similar and contain no ballistic regime. However, the emergence of a ballistic regime at times  $\tau_o \ll t \ll \bar{\tau}_R$  is evident in the latter case.

In what follows, we investigate the asymptotic behavior of the MSD for the case when  $\bar{D}_R \gg 1/\tau_o$ . To do so, we separate the relevant time scales in the

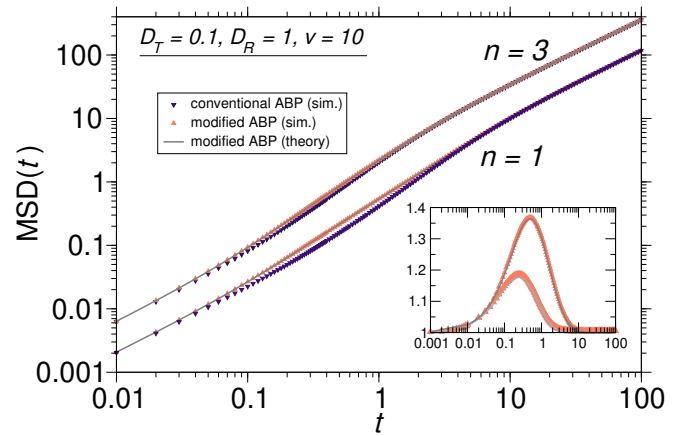


FIG. 1. Comparison of the MSDs for the ordinary ABP and the modified one with different number of the dimension for Ornstein-Uhlenbeck process. The parameters used here are  $v^* = 1$ ,  $D_R^* = 1$ , and  $D_T^* = 0.1$ . The qualitative behavior of the MSDs does not change by the fluctuations. The short and long time behavior of MSDs are in quantitative agreement, although a small quantitative deviation at intermediate times (the ballistic regime) is observed. The inset shows the ratio

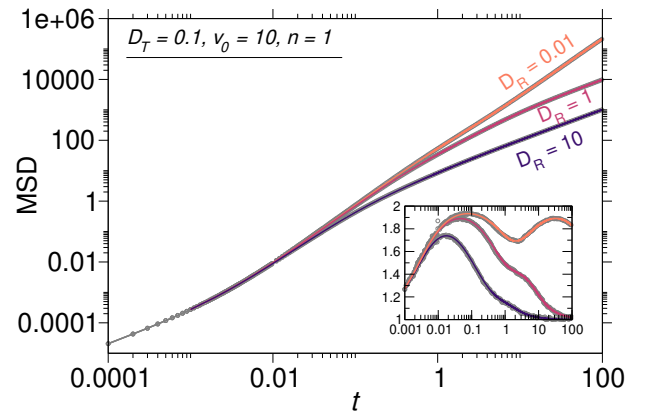


FIG. 2. Comparison of the MSD of the fluctuating ABP with different  $D_R^*$  values (with the equilibrium initial conditions). The gray symbols represent the simulation results and the lines represent the predictions of Eq. (15). The inset shows the exponent of the MSD calculated as  $\alpha = \frac{d \log \text{MSD}}{d \log t}$ .

$\Upsilon_n^{eq}(D_R^*, t)$ . For  $\bar{D}_R \gg 1/\tau_o$ , using the Taylor expansion as  $\frac{t}{\tau_o} \sqrt{1 + \frac{4\bar{D}_R\tau_o}{n}} \simeq \frac{t}{\tau_o} + \frac{2\bar{D}_R t}{n}$ , for the arguments of sinh and cosh functions in Eq. (14) and with some algebra we can obtain the asymptotic behavior of the MSD in different time-scales for  $n = 1$  as follows:

$$\langle r^2(t) \rangle \sim \begin{cases} 4\bar{D}_T t & t \ll \tau_o \ll \bar{\tau}_R \\ \bar{v}^2 t^2 & \tau_o \ll t \ll \bar{\tau}_R \\ 4(\bar{D}_T + \frac{\bar{v}^2}{2\bar{D}_R}) t & \tau_o \ll \bar{\tau}_R \ll t. \end{cases} \quad (16)$$

According to Eq. 16 the well-known behavior of the MSD of the ordinary ABP (see Eq. 11) is preserved when the

fluctuations are introduced in the equations of the motion. Nevertheless, the fluctuations only affect the cross-over from the linear regime at short times to the ballistic regime in the intermediate times. Our result here is complementary to the case, where the fluctuations arise internally which results in more complex dynamics [37].

We now proceed by investigating the behavior of the PDF of the particle displacement. Considering the PDF of the sub-ordinator process as in Eq. 14, we obtain the asymptotic behavior of the PDF for  $t \gg \bar{\tau}_R$  as

$$\hat{P}(\mathbf{k}, t) \sim \hat{\Upsilon}_n^{eq}(D' \mathbf{k}^2, t). \quad (17)$$

Following the discussion in Sec. II B 2, our asymptotic result concerning the PDF of the particle displacement is identical to the case of a passive Brownian particle under fluctuations [15], while the diffusion coefficient is substituted with the coarse-grained one being  $D' = \frac{v^{*2}}{2D_R^*} + D_T^*$ . Therefore, our analysis of the PDF is relevant only at times  $t > \tau_R^*$ . Nevertheless, if the characteristic time for the environmental fluctuations is longer than  $\tau_R^*$ , one can still capture the effect of fluctuations on the behavior of the PDF. In Fig. 3, we compare the form of the PDF for the conventional and the fluctuating ABPs. The form of the PDF for the conventional ABP remains Gaussian at all times. However, an exponential behavior of the PDF of displacement for the fluctuating ABP is observed at short times, despite the linear behavior of the MSD. This is the signature of the diffusing diffusivity model. For times longer than  $\tau_o$  the emergence of the Gaussian form of the PDF is evident. For a comprehensive asymptotic analysis of the PDF of particle displacement, we

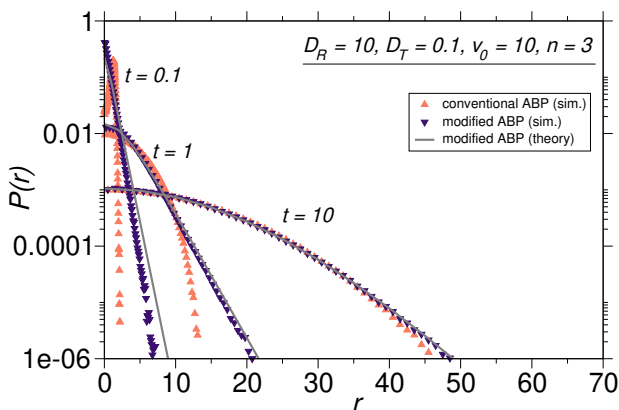


FIG. 3. Comparison of PDFs of conventional ABP and the modified one, corresponding to the MSDs depicted in Fig. (1) with  $n = 3$ .

*Non-equilibrium initial conditions:* Unlike the case with equilibrium initial conditions, here the process  $\mathbf{Y}$  at  $t = 0$  is not in its stationary state. An exemplary illustration of this situation would be to consider that the measurement starts as the particles are inserted in the

medium. In this case, the PDF of the particle displacement differs from the corresponding PDF for the equilibrium initial condition at short times. Nevertheless, as the time evolves the process  $\mathbf{Y}$  reaches its stationary state and one expects an identical behavior of the PDFs. Here, without loss of the generality, we assume the initial condition of  $\mathbf{Y}_0 = 0$ . In this case, the non-equilibrium PDF,  $\Upsilon_n^{neq}(u, t)$ , for the process  $u(t) = \int_0^t \Upsilon(t') dt'$  in the Laplace domain reads as [42]

$$\hat{\Upsilon}_n^{neq}(s, t) = \exp\left(\frac{nt}{2\tau_o}\right) \left[ \frac{1}{\sqrt{1 + 2s\sigma^2\tau_o^2}} \times \sinh\left(\frac{t}{\tau_o} \sqrt{1 + 2s\sigma^2\tau_o^2}\right) + \cosh\left(\frac{t}{\tau_o} \sqrt{1 + 2s\sigma^2\tau_o^2}\right) \right]^{n/2} \quad (18)$$

whose first moments is  $\langle u \rangle = \frac{n\sigma^2\tau_o}{2} (t - \frac{1}{2}\tau_o(1 - e^{-\frac{2t}{\tau_o}}))$ . This leads to a complex form for the MSD which widely differs from that for an ordinary ABP:

$$\langle r^2(t) \rangle = (4\bar{D}_T + 2\frac{\bar{v}^2}{D_R})(t - \frac{1}{2}\tau_o(1 - e^{-\frac{2t}{\tau_o}})) - 2\frac{\bar{v}^2}{D_R^2}(1 - \hat{\Upsilon}(D_R^*, t)). \quad (19)$$

Fig. 4 shows the plotted MSD according to Eq. 19 for  $\bar{c}$

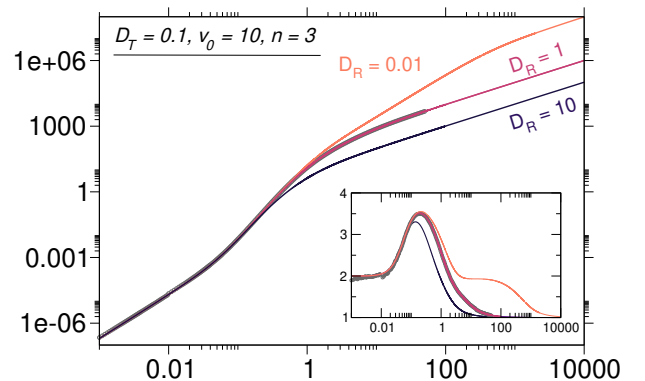


FIG. 4. Comparison of the MSD of the fluctuating ABP with different  $D_R^*$  values (with the non-equilibrium initial conditions). The gray symbols represent the simulation results and the lines represent the predictions of Eq. (19). The inset shows the exponent of the MSD.

In analogue to the previous section, we perform the asymptotic analysis of the MSD which yields:

$$\langle r^2(t) \rangle \sim \begin{cases} 4\bar{D}_T \frac{t^2}{\tau_o} & t \ll \tau_o \ll \bar{\tau}_R \\ \bar{v}^2 t^2 & \tau_o \ll t \ll \bar{\tau}_R \\ 4(\bar{D}_T + \frac{\bar{v}^2}{2D_R})t & \tau_o \ll \bar{\tau}_R \ll t. \end{cases} \quad (20)$$

The dynamics of the MSD at times shorter than  $\tau_o$  is now ballistic. This is explained by the initial acceleration due to the non-equilibrium initial condition. Apart

from that, at longer times,  $t \gg \tau_o$ , the expected ballistic behavior arising from the persistent motion of the ABP reappears as the times scales associated with the environmental fluctuations and the rotational relaxation deviate from each other. Finally, the linear behavior of the MSD at times  $t \gg \tau_o \gg \bar{\tau}_0$  emerges.

We further proceed by calculating the PDF of the particle displacement according to Eq. 18,  $\hat{P}(\mathbf{k}, t) \sim \hat{\Upsilon}_n^{neq}(D'\mathbf{k}^2, t)$ , at times longer and equal to the characteristic time for the environmental fluctuations ( $t_o = 1$ ). As seen in Fig. 5, the PDF at long times ( $t \gg t_o$ ) has a Gaussian from which exhibits a strong non-Gaussianity at shorter times ( $t \sim t_o$ ) which has widely been discussed in [14]. We note that the agreement between the theory and simulation results is not a surprise, as we have chosen the small values for  $t$ .

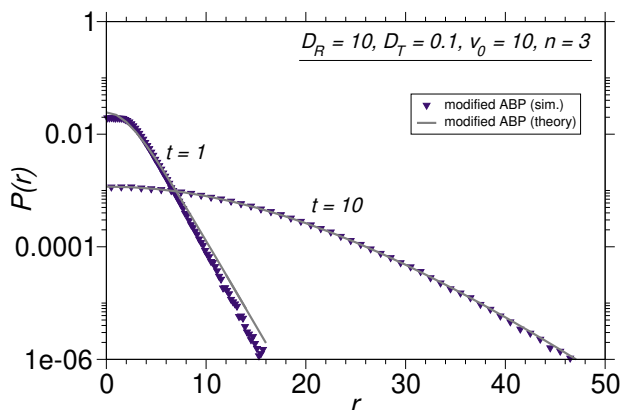


FIG. 5. PDF of the particle displacement at times longer and equal to the characteristic time for the fluctuations.

We finally note that the behaviour of the PDF of particle orientation,  $P(\phi, t)$ , is independent of the activity. Under the aforementioned fluctuations with an equilibrium initial conditions, it was shown [43] that  $P(\phi, t)$  exhibits exponential behaviour at times shorter than the characteristic time of the fluctuations and a Gaussian behaviour at longer times is recovered. In what follows, we will study the collective behaviour of the active matter constituted of the fluctuating ABPs. Here, we will discuss how these short times behaviours of PDFs of the rotational and translational displacements can alter the dynamic of the system.

### III. COLLECTIVE BEHAVIOR

Collectively the active particles show intriguing phenomena including self-ordered motion [44], motility-induced phase separation [45, 46], chemotaxis-induced dynamic clustering [47], and meso-scale turbulence [48–50], to name just a few. Here we focus on the well-studied phenomenon of motility-induced phase separation. In this study, as mentioned before, we extend the

original ABP model to include environmental fluctuations which affect the rotational and translational diffusivities together with the motility of each particle. Our study, in line with the recent studies of Refs. [51–53], is an attempt to model the active matter systems in a more realistic way. As the motility is a key ingredient of the MIPS, we expect a significant effect of the fluctuations on this phenomenon.

#### A. Simulation setup

We simulate the dynamics of the ABPs for an ensemble of particles and examine the collective behavior of these systems in absence and presence of the fluctuations.

As a special case, we first simulate the behavior of the system in the infinite dilution limit, i.e. the case where the interactions between the particles are negligible. In this limit, which we refer to as the single particle case, the dynamics of the particles are governed with Eqs. (3). These equations are integrated via the first order forward Euler scheme with time-step of  $\delta t = 10^{-3}$  for  $N \sim 10^6$  independent particles in an infinitely large two-dimensional plane. Particles are initially placed at the center of the plane, and the following equilibrium and non-equilibrium initial conditions for  $\mathbf{Y}$  are assigned to the particles. For the equilibrium case, the Ornstein-Uhlenbeck is simulated for each particle for  $10\tau_0$  and the obtained  $\mathbf{Y}$  values are used as the initial conditions. For the non-equilibrium initial conditions, as stated before, the initial conditions  $\mathbf{Y} = 0$  is used for all particles. Using these distributions for the initial conditions, Eqs. (3) are integrated to obtain  $\langle \mathbf{r}^2(t) \rangle$  and  $P(\mathbf{r}, t)$ , and the results are compared to the analytical predictions of in Sec. (II B 4).

To study the collective behavior of the system, an inter-particle interaction is introduced in Eqs. (3). A common choice of inter-particle potential to model the ABPs interactions is the soft purely repulsive and isotropic potential of Weeks-Chandler-Andersen [54] (WCA) which is  $V(\mathbf{r}) = 4\epsilon \left( \left( \frac{\sigma}{|\mathbf{r}|} \right)^6 - \left( \frac{\sigma}{|\mathbf{r}|} \right)^{12} \right)$  for  $|\mathbf{r}| \leq r_c = \sqrt[6]{2}$  and zero elsewhere, where  $\mathbf{r}$  is the distance between two particles,  $\sigma$  is associated diameter of the particle, and  $\epsilon$  is the energy scale of the interaction. The equations of motion for the  $i$ -th particle, in the dense regime read as,

$$\begin{aligned} \dot{\mathbf{r}}_i(t) &= v^* \Upsilon_i(t) \hat{\mathbf{e}}_i(t) + \sqrt{2D_T^* \Upsilon_i(t)} \boldsymbol{\xi}_{i,T}(t) + \frac{D_T^* \Upsilon_i(t)}{k_B T} \mathbf{F}_i \\ \dot{\phi}_i(t) &= \sqrt{2D_R^* \Upsilon_i(t)} \xi_{i,R}(t). \end{aligned} \quad (21)$$

where the vector  $\hat{\mathbf{e}}_i(t) := (\cos \phi, \sin \phi)$  is the heading direction of the  $i$ -th particle, and  $\mathbf{F}_i$  is the force on the  $i$ -th particle due to its interaction with all other particles.

In this work, we consider a system of  $N = 1600$  particles in a box with spatial extensions of  $L_x = L_y = 60\sigma$ , where the periodic boundary conditions are implemented along both  $x$  and  $y$ -directions. Following

Refs. [46, 52, 55, 56], we choose  $\sigma = 1$ , and  $\epsilon \gg k_B T$  such that which mimics the hard-core interaction. Note that the force,  $\mathbf{F}_i$ , enters the dynamics of the particle with a prefactor  $D_T^* \mathcal{Y}_i(t)/(k_B T)$  [see Eqs. (21)]. This prefactor does not play any role for a truly hard-core interaction, where the force is either zero (where there is no overlap) or infinite (in the case of an overlap). Nevertheless, as the implemented potential in our study only mimics the true hard-core interaction, this prefactor plays an important role: the particles are effectively softer when they have smaller translational diffusion. This is particularly important as there a high probability for small values of diffusion coefficients for the chosen random process of  $\mathcal{Y}_i(t)$ . To avoid this undesired deviation of  $\mathbf{F}_i$  from the hard-core interaction, we set  $\epsilon$  of the potential such that  $D_T^* \mathcal{Y}_i(t)\epsilon/(k_B T) = 100$  for all the particles and for all times. This way we avoid the undesired softening of the particles, which is known to hinder the MIPS. It is worth mentioning that with these choice of parameters, our reduced interaction energy  $\epsilon/(k_B T)$  is two orders of magnitude larger than the previous studies [], which leads to formation of more stable structures. The time integration of the resulting equations is performed using the first order forward Euler scheme with a much smaller time-step compared to the single particle simulations,  $\delta t = 10^{-5}$ , to avoid large overlap of the effective hard-disks [56]. Initially, the particles are positioned on a regular square lattice and the system is simulated for  $t = 50$  in Lennard-Jones time-units to reach its steady-state. All the measurements begin after this transient regime. To obtain reasonable statistics,  $N_s = 5$  independent samples are considered.

We study the phase separation in our system by analyzing the probability distribution of the local density across the system. To obtain the local density, we first calculate the area associated with each particle,  $A_i$ , using Voronoi tessellation [57], where index  $i$  refers to the particle IDs. The local density associated the  $i$ -th particle reads as  $\rho_i = 1/A_i$ , which corresponds to the particle resolved local packing fraction defined by  $\phi_i := \pi\sigma^2/(4A_i)$ . The probability of having local density  $\rho$  at any chosen point in the plain,  $\mathbf{r}$ , is proportional to the number of particles with  $\rho_i = \rho$  weighted by the area associated with each of those particles (i.e.  $A_i$ ). In this way one can obtain a probability distribution of the local density associated with position (and not particles). This method is equivalent to the procedure suggested in Ref. [56] with an infinitesimally small lattice spacing. We also use  $\rho_i$  to obtain the density dependent of the particle velocity. The velocities are calculated by the displacement of particles,  $\mathbf{v}_i(t) := (\mathbf{r}_i(t + \Delta t) - \mathbf{r}_i(t - \Delta t))/(2\Delta t)$ , where  $\Delta t$  is chosen to be 0.01 time units. This interval is large enough to average out the instantaneous thermal fluctuations (i.e. during 20 time-steps), but still small enough that the particles do not move significantly compared to its size (a displacement of  $v_0 \Delta t = 0.1$  is expected if a particle moves ballistically without any collision).

## B. Motility-induced phase separation

In Fig. (6), the phase diagram of the conventional and the modified ABP is presented. Two snapshots of the conventional ABP model are also shown together with a corresponding modified ABP snapshot in the inset of Fig. (6). The results clearly show that introducing fluctuations hinders the MIPS. This can be understood by considering the effect of the fluctuations on the commonly suggested microscopic mechanism of the MIPS [46]. The basic mechanism for the MIPS to occur is that two particles block each other's path over a time interval which is required for the other particles to reach this configuration. This forms a nucleus for the clustering to start [46]. The aforementioned time interval during which two particles are facing towards each other is obtained from the short time behaviour of PDF of particle orientational displacements. While for the conventional ABPs this distribution is governed by a Gaussian PDF, for the fluctuating ABP the short time distribution of the rotational displacements is an exponential function [43]. This means that in the same time interval the fluctuating ABPs explore larger angles. Thus fluctuating ABPs are more likely to avoid forming a cluster, which leads to hindrance of the MIPS. Qualitatively speaking, this means that, due to fluctuations, the collisions are less effective in slowing down the particles. As discussed in the next section, this is also in line with our observation that for any local density the ABPs have larger velocities in fluctuating model compared to the conventional one.

So far we have argued about the possible microscopic effect of the fluctuations on the cluster formation. Interestingly, the snapshots in Fig. (6) suggest that when the dense phase is formed in presence of the fluctuations, the structure of its boundary is less sharp compared to the boundaries of the clusters formed in the corresponding conventional ABP system. This can be explained again by considering the short time behaviour of the translational and rotational displacements PDFs. Here, one should focus on the behavior of the particles which are right at the boundary or the particles inside the cluster which are close to the boundary. These are the particle might find their way out of the cluster by exploring the possible ways out of the cluster. Roughly speaking, by rotating faster and performing larger displacements (as reflected in the exponential distributions of the rotational and translational displacements at short times) the particles in the fluctuating model find their way out of the cluster faster compared to the ABPs in the conventional model.

A more detailed analysis of particle velocity distribution inside and outside of the cluster is presented in the followings where we study the correlation between the particle densities and the velocities.

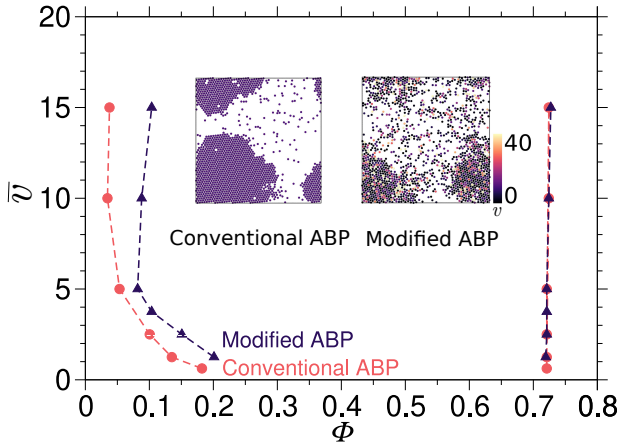


FIG. 6.  $D_R^* = 0.1$ ,  $D_T^* = 0.001$ ,  $v^* = 10$ ,  $n = 1$ ,  $\sigma_o = 1$ ,  $\bar{\Phi} = 0.44$ . A snapshot of the simulation for conventional ABP (up-left panel), and a snapshot of the corresponding diffusive activity ABP model (up-right panel). The color code shows the local density obtained by Voronoi-tessellation; the darker color shows denser environment. The snapshots are suggestive of larger and more stable dense phase for the conventional ABP compared to the active diffusivity model. The destructive behavior of introducing fluctuation on motility induced phase separation.

### C. Density dependent distribution of velocities

A better insight into the effect of the fluctuations on the MIPS can be gained by analyzing the dependence of particle velocities on the local density. This dependency is shown in Fig. (7) for systems in presence and absence of the fluctuations. Our results show that the fluctuations not only hinders the MIPS, but also it lead to a significant change in the dependency of the velocity on the density. To shed light on these effects, we divide each curve in Fig. (7) into four density intervals (indicated by the Roman numbers) and discuss the behavior of the system in each interval. A representative snapshot for each system is also presented in Fig. (7), where particles with densities corresponding to each interval are colored differently. Using these snapshots one can find the positions of the particles belonging to each density interval.

As a general remark on the shape of  $v(\rho)$  curve for the conventional ABPs, we point out that in our study the dependency of  $v$  on  $\rho$  is not a linear function, in contrast to the common observation of the linear dependency. This qualitative difference is due to choosing a relatively low  $D_T$ , and a relatively large  $\epsilon$ , in our study. The motivation to choose a larger  $\epsilon$  is to achieve a better representation of the hard-disk. Although the translation diffusion coefficient is commonly estimated to be of the same order of magnitude as  $\sigma^2 D_R$ , in our study we effectively ignored the effect of  $D_T$  by setting it to a value two orders of magnitude smaller than the aforementioned estimate.

In the dilute limit, i.e. for  $\rho_i \rightarrow 0$ , particle velocities

are equal to the average velocity, both in absence and presence of the fluctuations. By increasing density from zero, the particles hinder each other's motion via collisions, which leads to a deviation of the velocities from the single particle case. The particle velocity is monotonically decreasing with the particle density in the range (I) for both systems. In this regime, where particles are mainly in the dilute phase, the slowing down is weaker for the system with fluctuations. The fluctuations (which are density-independent) randomize the particle velocities irrespective of their local densities, which counteracts the (density-dependent) effect of collisions. In this way, the particle dynamics becomes less sensitive to the local density and therefore the extent of the density of the dilute phase is extended to larger densities, where the collisions become more frequent. This is also in line with our previous argument about hindrance of the cluster formation due to existing fluctuations.

Next, we investigate the more dense regions (i.e. the ranges (II)–(IV)) which form the boundary and the bulk of the cluster, as well as the defects. The snapshots suggest that the particles in the range (II) are commonly on the boundary of the formed clusters. In this density range, the velocity decreases monotonically by increasing density. This monotonic decrease of the velocity is changed in the density range (III). Interestingly, a local minimum is observed at  $\rho_i = 0.62$ . Investigating the particles in corresponding density region shows that these particles belong to the following groups: the particles on the boundary, or the particles around the isolated point defects inside the cluster. The estimated density associated with the latter group is  $6/7\rho_i^c = 0.62$  where  $\rho_i^c = 0.72$  is the largest packing fraction of the system. This estimate coincides with the location of the minimum, which confirms our observation that this density corresponds to the aforementioned groups. The velocity associated with this density is consequently an average of the velocities of particles in these groups; the almost zero velocity of the latter group leads the appearance of this local minimum at this particular density. With further increase of the density, we enter the most dense range, i.e. the regime (IV) which corresponds to the density of particles which are closely packed inside the cluster (see the corresponding snapshots). In this regime, the particle velocities are almost zero irrespective of the presence of fluctuations and the two curves in Fig. (7) merge.

Using the dependency of  $v$  on  $\rho$  one can find the (so-called) effective free energy of the system as a function the packing fraction [58],  $f(\rho)$ . The proposed effective free energy is composed of two contribution, the bulk contribution,  $f_0$ , and the contribution due to the repulsive interaction of the particles (which mimicks the excluded volume effects),  $f_{\text{rep}}$ :

$$f(\rho) = f_0(\rho) + f_{\text{rep}}(\rho), \quad (22)$$

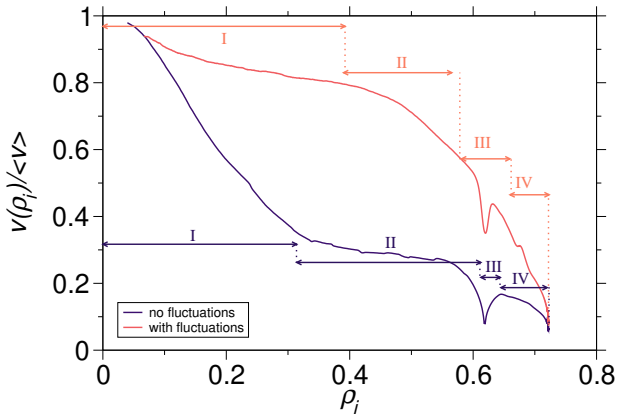


FIG. 7. Upper panel: velocity as a function of particle density for  $D_R^* = 0.1$ ,  $D_T^* = 0.001$ ,  $v^* = 10$ ,  $n = 1$ . Lower panel: Representative snapshots of the systems with and without fluctuations (right and left pictures, respectively). Particles color-code based on their density,  $\rho_i$ , with red [range (I)], yellow [range (II)], blue [range (III)], and gray [range (IV)] colors.

with

$$f_0(\rho) = \rho(\ln \rho - 1) + \int_0^\rho \ln[v(\rho)] d\rho, \quad (23)$$

$$f_{rep}(\rho) = k_{rep} \Theta(\rho - \rho_t)(\rho - \rho_t)^4. \quad (24)$$

where  $\Theta$  is the Heaviside function.  $k_{rep}$  is a large constant, and  $\rho_t$  is the threshold density, which are both potential dependent parameters. The choice of  $\rho_t$  is guided by the largest density values occurring in the system (see Fig. (6)). Using these parameters, we have calculated the free energy as a function of density (see Fig. (8)) and obtained the coexistence densities via the common tangent construction. The obtained coexistence densities (which are depicted in Fig. (6) using cross symbols) show that the density associated with the dense phase is not affected by the fluctuations and in contrary to that the density of the dilute phase is shifted to larger values due to the fluctuations. This is in line with the observed effect of the fluctuations in Fig. (6).

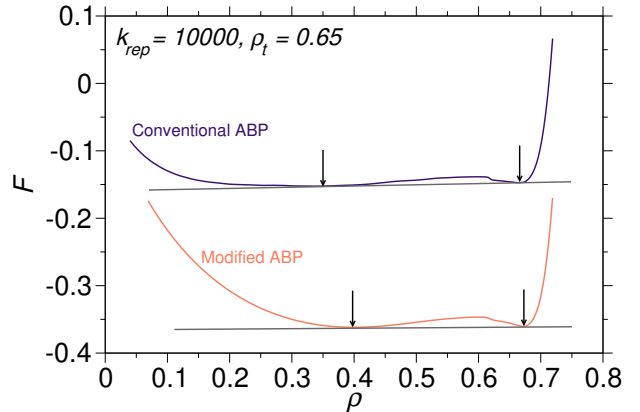


FIG. 8. The effective free energy as a function of the density for a modified ABP system with  $D_R^* = 0.1$ ,  $D_T^* = 0.001$ ,  $v^* = 10$ ,  $n = 1$ , and the corresponding system without fluctuations. The dashed lines represent the common tangent line. One should note that for clarity the free energies are modified by adding linear terms in  $\rho$  which are irrelevant for the common tangent construction.

#### IV. CONCLUSIONS

In this work we studied the impact of fluctuations on the dynamics of the single ABPs as well as their collective behaviour. The fluctuations are introduced to model an evolving environment in which the particle diffuses and explores regions with different viscosities. This is essentially the idea of diffusing diffusivity model. More specifically, we assumed that the motility, rotational and the translational diffusivities fluctuate simultaneously according to a random process that mimics the heterogeneity of the system. Using the sub-ordination concept, we obtained the exact form of the MSD and the asymptotic behaviour of the PDF of particle displacement for a general random process. We continued by calculating the explicit forms of the MSD and the PDF of particle displacements assuming the square Ornstein-Uhlenbeck process with two different initial conditions of the fluctuating process, namely the equilibrium and the non-equilibrium initial conditions. We showed that, similar to the case of passive particles, the PDF of particle displacements exhibits an exponential behaviour at short times compared to the characteristic time of the fluctuation. At longer times, the Gaussian form of the distribution is recovered. The MSD of the fluctuating ABP preserves the original ballistic and linear regimes as in the ordinary ABP, however, a complicated form of cross-overs appear when the characteristic time for the fluctuations is much shorter than the rotational relaxation time. We performed particle based simulations of the modified ABPs to confirm the obtained analytical results. We found quantitative agreement between the simulation results and the predicted analytical behavior of the single particles.

We proceeded by investigating the impact of these fluctuations on the collective behaviour of the system

using particle based ABP simulations. We focused on the motility induced phase separation phenomenon which typically occurs for ordinary ABPs. We calculated the phase diagram of motility-density for the modified ABP system and compared it with that for the ordinary system. A considerable shift at the phase diagram suggests that highly transient clusters with small sizes appears which can alter the size distribution of cluster. We also observed that the MIPS in the fluctuating system takes place at much longer times than the non-fluctuating sys-

tem. The structure of the formed clusters contain more roughness on the boundaries as well as disorders in the body of the formed clusters in the modified ABP system. Using our theoretical results, we argued that these observations in the collective system are mainly due to the short time behaviour of the PDF of the translational and the rotational displacements. To support our discussion, we studied the density dependent of the particle velocity, which shows that introducing the fluctuations leads to less effective hindrance of the particles due to collisions.

- 
- [1] I. M. Sokolov, *Soft Matter*, 2012, **8**, 9043–9052.
- [2] B. Wang, S. M. Anthony, S. C. Bae and S. Granick, *Proc. Natl. Acad. Sci. U. S. A.*, 2009, **106**, 15160.
- [3] J. Guan, B. Wang and S. Granick, *ACS Nano*, 2014, **8**, 3331.
- [4] B. Wang, J. Kuo, S. C. Bae and S. Granick, *Nat. Mater.*, 2012, **11**, 481.
- [5] W. K. Kegel and A. van Blaaderen, *Science*, 2000, **287**, 290.
- [6] G. Kwon, B. J. Sung and A. Yethiraj, *J. Phys. Chem. B*, 2014, **118**, 8128g.
- [7] J. Kim, C. Kim and B. J. Sung, *Phys. Rev. Lett.*, 2013, **110**, 047801.
- [8] R. Metzler, *Biophys. J.*, 2017, **112**, 413.
- [9] C. Beck and E. G. Cohen, *Physica A*, 2003, **322**, 267.
- [10] M. V. Chubynsky and G. W. Slater, *Phys. Rev. Lett.*, 2014, **113**, 098302.
- [11] R. Jain and K. L. Sebastian, *J. Phys. Chem. B*, 2016, **120**, 3988.
- [12] R. Jain and K. L. Sebastian, *J. Phys. Chem. B*, 2016, **120**, 9215.
- [13] Y. Lanoiselée and D. S. Grebenkov, *J. Phys. A*, 2018, **51**, 145602.
- [14] V. Sposini, A. V. Chechkin, F. Seno, G. Pagnini and R. Metzler, *New J. Phys.*, 2018, **20**, 043044.
- [15] A. V. Chechkin, F. Seno, R. Metzler and I. M. Sokolov, *Phys. Rev. X*, 2017, **7**, 021002.
- [16] S. Khadem and I. Sokolov, *Phys. Rev. E*, 2017, **95**, 052139.
- [17] B. Alberts, D. Bray, J. Lewis, M. Raff, K. Roberts and J. Watson, *Molecular Biology of the Cell*, Garland, 1994.
- [18] M. Dworkin, *Mycobacteria II (Amer Society for Microbiology)*, 1993.
- [19] R. M. Holdo, J. M. Fryxell, A. R. Sinclair, A. Dobson and R. D. Holt, *PLoS One*, 2011, **6**, e16370.
- [20] O. Chepizhko and F. Peruani, *Eur. Phys. J. Special Topics*, 2015, **224**, 1287.
- [21] O. Chepizhko, E. G. Altmann and F. Peruani, *Phys. Rev. Lett.*, 2013, **110**, 238101.
- [22] D. A. Quint and A. Gopinathan, *Phys. Biol.*, 2015, **12**, 046008.
- [23] M. Zeitz, K. Wolff and H. Stark, *Eur. Phys. J. E*, 2017, **40**, 23.
- [24] O. Chepizhko and F. Peruani, *Phys. Rev. Lett.*, 2013, **111**, 160604.
- [25] C. O. Reichhardt and C. Reichhardt, *New Journal of Physics*, 2018, **20**, 025002.
- [26] C. Reichhardt and C. O. Reichhardt, *Physical Review E*, 2018, **97**, 052613.
- [27] C. Bechinger, R. Di Leonardo, H. Löwen, C. Reichhardt, G. Volpe and G. Volpe, *Rev. Mod. Phys.*, 2016, **88**, 045006.
- [28] B. ten Hagen, S. van Teeffelen and H. Löwen, *J. Phys.: Condens. Matter*, 2011, **23**, 194119.
- [29] J. R. Howse, R. A. Jones, A. J. Ryan, T. Gough, R. Vafabakhsh and R. Golestanian, *Phys. Rev. Lett.*, 2007, **99**, 048102.
- [30] F. Kümmel, B. ten Hagen, R. Wittkowski, I. Buttinoni, R. Eichhorn, G. Volpe, H. Löwen and C. Bechinger, *Phys. Rev. Lett.*, 2013, **110**, 198302.
- [31] C. Kurzthaler, C. Devailly, J. Arlt, T. Franosch, W. C. Poon, V. A. Martinez and A. T. Brown, *Phys. Rev. Lett.*, 2018, **121**, 078001.
- [32] H. Löwen, *arXiv preprint arXiv:1910.13953*, 2019.
- [33] S. van Teeffelen and H. Löwen, *Phys. Rev. E*, 2008, **78**, 020101.
- [34] J. Bialké, T. Speck and H. Löwen, *Phys. Rev. Lett.*, 2012, **108**, 168301.
- [35] I. Buttinoni, J. Bialké, F. Kümmel, H. Löwen, C. Bechinger and T. Speck, *Phys. Rev. Lett.*, 2013, **110**, 238301.
- [36] G.-J. Liao and S. H. Klapp, *Soft Matter*, 2018, **14**, 7873.
- [37] F. Peruani and L. G. Morelli, *Phys. Rev. Lett.*, 2007, **99**, 010602.
- [38] S. Bochner, *Harmonic analysis and the theory of probability*, Courier Corporation, 2005.
- [39] A. Weron and M. Magdziarz, *EPL*, 2009, **86**, 60010.
- [40] F. Thiel, F. Flegel and I. M. Sokolov, *Phys. Rev. Lett.*, 2013, **111**, 010601.
- [41] F. J. Sevilla and M. Sandoval, *Phys. Rev. E*, 2015, **91**, 052150.
- [42] T. Dankel, Jr, *SIAM J. Appl. Math*, 1991, **51**, 568.
- [43] R. Jain and K. Sebastian, *J. Chem. Phys.*, 2017, **146**, 214102.
- [44] T. Vicsek, A. Czirók, E. Ben-Jacob, I. Cohen and O. Shochet, *Phys. Rev. Lett.*, 1995, **75**, 1226.
- [45] J. Stenhammar, A. Tiribocchi, R. J. Allen, D. Marenduzzo and M. E. Cates, *Phys. Rev. Lett.*, 2013, **111**, 145702.
- [46] I. Buttinoni, J. Bialké, F. Kümmel, H. Löwen, C. Bechinger and T. Speck, *Phys. Rev. Lett.*, 2013, **110**, 238301.
- [47] I. Theurkauff, C. Cottin-Bizonne, J. Palacci, C. Ybert and L. Bocquet, *Phys. Rev. Lett.*, 2012, **108**, 268303.
- [48] H. H. Wensink, J. Dunkel, S. Heidenreich, K. Drescher, R. E. Goldstein, H. Löwen and J. M. Yeomans, *Proc. Natl. Acad. Sci. U. S. A.*, 2012, **109**, 14308.
- [49] H. Reinken, S. H. Klapp, M. Bär and S. Heidenreich,

- Phys. Rev. E*, 2018, **97**, 022613.
- [50] H. Reinken, S. Heidenreich, M. Bär and S. H. Klapp, *New J. Phys.*, 2019, **21**, 013037.
- [51] S. N. Weber, C. A. Weber and E. Frey, *Phys. Rev. Lett.*, 2016, **116**, 058301.
- [52] A. Fischer, A. Chatterjee and T. Speck, *J. Chem. Phys.*, 2019, **150**, 064910.
- [53] R. Van Damme, J. Rodenburg, R. Van Roij and M. Dijkstra, *J. Chem. Phys.*, 2019, **150**, 164501.
- [54] J. D. Weeks, D. Chandler and H. C. Andersen, *J. Chem. Phys.*, 1971, **54**, 5237.
- [55] J. T. Siebert, J. Letz, T. Speck and P. Virnau, *Soft Matter*, 2017, **13**, 1020.
- [56] G.-J. Liao and S. H. Klapp, *Soft Matter*, 2018, **14**, 7873.
- [57] C. H. Rycroft, *Chaos*, 2009, **19**, 041111.
- [58] J. Tailleur and M. Cates, *Phys. Rev. Lett.*, 2008, **100**, 218103.

This figure "all-ranges.png" is available in "png" format from:

<http://arxiv.org/ps/2103.16582v1>

This figure "combined-no-fluctuations.png" is available in "png" format from:

<http://arxiv.org/ps/2103.16582v1>